Proc. Natl. Sci. Counc. ROC(A)
Vol. 20, No. 1, 1996. pp. 118-122

(Scientific Note)

Full-Wave Analysis of Cylindrical Microstrip Open-End Discontinuities

KIN-LU WONG, HUA-MING CHEN, AND RUENN-BO TSAI

Department of Electrical Engineering
National Sun Yat-Sen University
Kaohsiung, Taiwan, R.O.C.

(Received March 18, 1995; Accepted July 22, 1995)

ABSTRACT

This paper presents a full-wave solution for the characteristics of cylindrical microstrip open-end discontinuities. Numerical results are obtained using the exact Green's function in a moment-method calculation. Results for the frequency-dependent reflection coefficient from the open-end discontinuity are presented, and the equivalent terminal conductance and capacitance for the open-end discontinuity are also evaluated and discussed.

Key Words: cylindrical microstrip line, microstrip discontinuity

I. Introduction

The study of cylindrical microstrip discontinuities is important for applications involving microwave and millimeter-wave integrated circuits on cylindrical surfaces. Such cylindrical microstrip circuits can be used as feeding circuitry for cylindrical microstrip patch antennas (Ke and Wong, 1994) employed on high-speed aircraft and missiles. Recently, many studies treating microstrip discontinuities on planar geometries (Alexopoulos and Wu, 1994; Harokopus *et al.*, 1991; Kobayashi and Sekine, 1991; Yang *et al.*, 1989; Jackson and Pozar, 1985) have been published; however, very scant information is available in the literature on cylindrical microstrip discontinuities. In this paper, the analysis of a cylindrical microstrip open-end discontinuity is presented. A rigorous full-wave analysis using a Green's-function formulation is performed, and the results are calculated using a moment-method calculation. The reflection coefficients from the open-end discontinuity for different curvilinear coefficients, defined as the ratio of the inner to outer radii, i.e., $R=a/b$ (Alexopoulos and Nakatani, 1987), are calculated. Results for a larger value of R are also compared with that of a planar open-end discontinuity (Alexopoulos and Wu, 1994) to ascertain the numerical calculation. The equivalent terminal conductance and capacitance at the open-end discontinuity are also evaluated and discussed.

II. Theory

Figure 1 shows the geometry of a cylindrical microstrip open-end discontinuity. The microstrip line

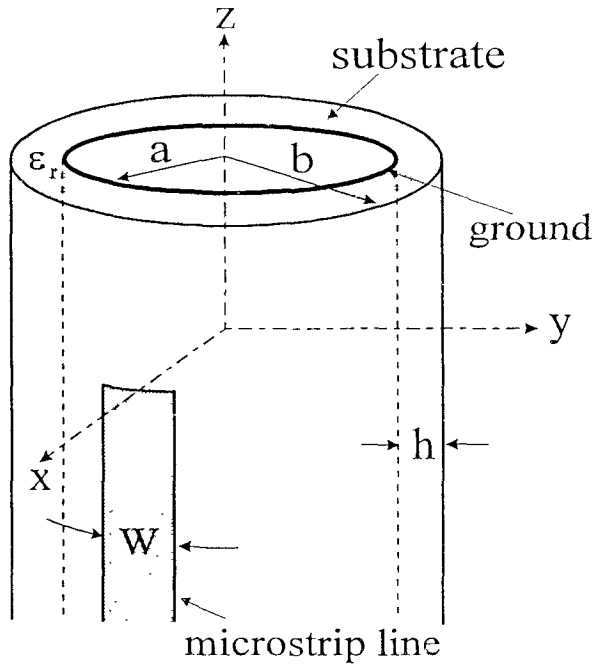

Fig. 1. The geometry of a cylindrical microstrip open-end discontinuity.

with width W has an open-end discontinuity at z=0 and is of infinite length in the -$\hat{z}$ direction. The cylindrical grounded substrate has a thickness h (=b-a) and a relative permittivity ε_r. The outer medium is air with permittivity ε_0 and permeability μ_0. To begin with, the current density on the microstrip line is modeled. For the current far away from the open-end, a traveling-wave of the form $\overline{J}(\phi,z)=\hat{z}f(\phi)\exp(-j\beta z)$ is assumed, where β is the effective propagation constant of the microstrip line with infinite length, and $f(\phi)$ is chosen to be uniform. This assumption is adequate when the width and substrate thickness of the microstrip line are much less than the operating wavelength (Jackson and Pozar, 1985; Yang *et al.*, 1989). In this case, the propagation constant, β, which is required for the solution of an open-end microstrip line, can be solved for by imposing a boundary condition that the electric field must vanish on the microstrip line. Thus, β can be obtained by solving

$$\sum_{p=-\infty}^{\infty} \tilde{G}_{zz}(b, p, \beta)\, \tilde{f}(p)\, \tilde{f}(-p) = 0 \tag{1}$$

with

$$\tilde{f}(p) = \frac{1}{b}\frac{\sin p\phi_0}{p\phi_0}, \quad \phi_0 = \frac{W}{2b}, \tag{2}$$

$$\tilde{G}_{zz}(b, p, \beta) = \frac{j\eta k_{2\rho}}{D_p k_0}\left[\frac{H_p^{(2)\prime}(k_{2\rho}b)}{H_p^{(2)}(k_{2\rho}b)} X_p^{(2)} - \frac{k_{2\rho}}{k_{1\rho}}\right], \tag{3}$$

$$D_p = \left[\frac{H_p^{(2)\prime}(k_{2\rho}b)}{H_p^{(2)}(k_{2\rho}b)} - \varepsilon_r X_p^{(1)}\frac{k_{2\rho}}{k_{1\rho}}\right]\left[X_p^{(2)}\frac{H_p^{(2)\prime}(k_{2\rho}b)}{H_p^{(2)}(k_{2\rho}b)} - \frac{k_{2\rho}}{k_{1\rho}}\right] - \left[(\varepsilon_r - 1)\frac{p\beta k_0}{bk_{1\rho}^2 k_{2\rho}}\right]^2 X_p^{(2)},$$

$$X_p^{(1)} = \frac{H_p^{(2)}(k_{1\rho}a) J_p'(k_{1\rho}b) - J_p(k_{1\rho}a) H_p^{(2)\prime}(k_{1\rho}b)}{H_p^{(2)}(k_{1\rho}a) J_p(k_{1\rho}b) - J_p(k_{1\rho}a) H_p^{(2)}(k_{1\rho}b)},$$

$$X_p^{(2)} = \frac{H_p^{(2)\prime}(k_{1\rho}a) J_p(k_{1\rho}b) - J_p'(k_{1\rho}a) H_p^{(2)}(k_{1\rho}b)}{H_p^{(2)\prime}(k_{1\rho}a) J_p'(k_{1\rho}b) - J_p'(k_{1\rho}a) H_p^{(2)\prime}(k_{1\rho}b)},$$

$$k_0 = \omega\sqrt{\mu_0\varepsilon_0}, \quad \eta = \sqrt{\mu_0/\varepsilon_0},$$

$$k_{1p}^2 = \varepsilon_r k_0^2 - \beta^2, \quad k_{2p}^2 = k_0^2 - \beta^2,$$

where $\tilde{G}_{zz}(b, p, \beta)$, a Green's function in the spectral domain, denotes the $\hat{z}$-directed electric field at ρ=b due to a unit of $\hat{z}$-directed current at (b, ϕ, z), and $\tilde{f}(p)$ is the Fourier transform of $f(\phi)$; $H_p^{(2)}(x)$ is a Hankel function of the second kind with order p, and $J_p(x)$ is a Bessel function of the first kind with order p. The prime in the equation denotes a derivative with respect to the argument.

Next, the current density near the open-end is modeled as (Yang *et al.*, 1989; Jackson and Pozar, 1985)

$$\overline{J}(\phi,z) = \hat{z}f(\phi)g(z) \tag{4}$$

with

$$g(z) = (1-\Gamma)f_s(\beta z+\pi/2) - j(1+\Gamma)f_s(\beta z) + \sum_{n=1}^{N} I_n g_n(z), \quad z\le 0, \tag{5}$$

$$I_n g_n(z) = I_n \frac{\sin\beta(d-|z-z_n|)}{\sin\beta d}, \quad |z-z_n| < d,$$

$$z_n = -nd, \; n=1, 2, 3, \ldots, \tag{6}$$

$$f_s(u) = \begin{cases} \sin u, & 0 > u > -m\pi, \\ 0, & \text{elsewhere}, \end{cases} \tag{7}$$

where Γ is the reflection coefficient from the discontinuity at z=0; $g(z)$ is a piecewise sinusoidal basis function chosen to represent currents that are the higher-order propagating modes; I_n are the unknown expansion coefficients for the PWS function, and d is the half-length of the PWS mode. The sinusoidal functions of Eq. (7), chosen to be several (m/2) circles in length (Jackson and Pozar, 1985), represent the incident and reflected traveling waves of the fundamental propagation mode.

To solve for the unknown expansion coefficient, I_n, the boundary condition that the electric field on the microstrip line must be zero is again applied, which yields

$$0 = \int_{-\infty}^{0}\int_{-\phi_0}^{\phi_0} G_{zz}(\phi, z) J(\phi, z)\, d\phi dz = \frac{1}{2\pi}\sum_{p=-\infty}^{\infty}\int_{-\infty}^{\infty} \tilde{G}_{zz}(b, p, k_z)\tilde{J}(p, k_z) e^{-j(p\phi + k_z z)} dk_z \tag{8}$$

with

$$\tilde{J}(p, k_z) = \tilde{f}(p)\left[(\tilde{f}_c - j\tilde{f}_s) - \Gamma(\tilde{f}_c + j\tilde{f}_s) + \sum_{n=1}^{N} I_n \tilde{g}_n\right]. \tag{9}$$

In the equations above, $\tilde{g}_n$, $\tilde{f}_s$, and $\tilde{f}_c$ are the Fourier transforms of g_n, $f_s(\beta z)$, and $f_s(\beta z+\pi/2)$, respectively, and are given as

$$\tilde{g}_n(k_z) = \frac{2\beta(\cos k_z d - \cos\beta d)}{\sin\beta d\,(\beta^2 - k_z^2)} e^{jk_z z_n}, \tag{10}$$

$$\tilde{f}_s(k_z) = \frac{\beta}{(k_z^2 - \beta^2)}[1 - (-1)^m e^{-jm\pi k_z/\beta}], \tag{11}$$

$$\tilde{f}_c(k_z) = e^{-jk_z\pi/2\beta}\tilde{f}_s(k_z).$$

Then, by following Galerkin's procedure described in Jackson and Pozar (1985), the integral equation in Eq. (8) can be converted into a matrix equation:

$$[Z_{mn}]_{(N+1)\times N}\,[-(Z_{mc} + jZ_{ms})]_{(N+1)\times 1}\begin{bmatrix}[I_n]_{N\times 1}\\ \Gamma\end{bmatrix}$$

$$= [-Z_{mc} + jZ_{ms}]_{(N+1)\times 1} \tag{12}$$

with

$$Z_{mn} = \sum_{p=-\infty}^{\infty}\int_{-\infty}^{\infty}\tilde{G}_{zz}(b, p, k_z)\,\tilde{f}^2(p)\,\tilde{g}_m(-k_z)\,\tilde{g}_n(k_z)\,dk_z, \tag{13}$$

$$Z_{ms} = \sum_{p=-\infty}^{\infty}\int_{-\infty}^{\infty}\tilde{G}_{zz}(b, p, k_z)\,\tilde{f}^2(p)\,\tilde{g}_m(-k_z)\,\tilde{f}_s(k_z)\,dk_z, \tag{14}$$

$$Z_{mc} = \sum_{p=-\infty}^{\infty}\int_{-\infty}^{\infty}\tilde{G}_{zz}(b, p, k_z)\,\tilde{f}^2(p)\,\tilde{g}_m(-k_z)\,\tilde{f}_c(k_z)\,dk_z. \tag{15}$$

By solving Eq. (12), the reflection coefficient Γ and the coefficients I_n for the PWS expansion functions can be obtained. Once Γ is calculated, an open-end admittance Y can be defined as

$$Y = \frac{1-\Gamma}{Z_0(1+\Gamma)} = G + j\omega C_0, \tag{16}$$

where Z_0 is the characteristic impedance of the cylindrical microstrip line and can be calculated using the theoretical approach described by Alexopoulos and Nakatani (1987); G is the open-end conductance, and C_0 is the open-end capacitance. That is, the open-end discontinuity can be characterized by an equivalent circuit with a terminal conductance and a terminal capacitance as shown in Fig. 2. The conductance accounts for the radiation and surface wave losses, and the capacitance is due to the fringing electric field at the open-end. Results of the reflection coefficient and the open-end admittance for a cylindrical open-end microstrip line with various parameters have been calculated and analyzed.

III. Numerical Results and Discussion

Figure 3 shows the reflection coefficient magnitude at a cylindrical microstrip open-end discontinuity with different curvilinear coefficients. In the calculation, four PWS functions in Eq. (6) and six cycles of the sinusoidal functions in Eq. (7) were used for the expansion of the current on the microstrip line, which results in good convergent solutions. From the results, it is found that the curvature effect on the reflection coefficient magnitude is significant. It is also observed that the reflection coefficient magnitude decreases when the curvature increases (i.e., the value of R decreases). However, as for the phase of the reflection coefficient, the obtained results show very small variations for different values of R and are not presented for brevity.

Figure 4 shows the results of the equivalent terminal conductance for an open-end microstrip discontinuity with R=0.8. The planar results (Alexopoulos

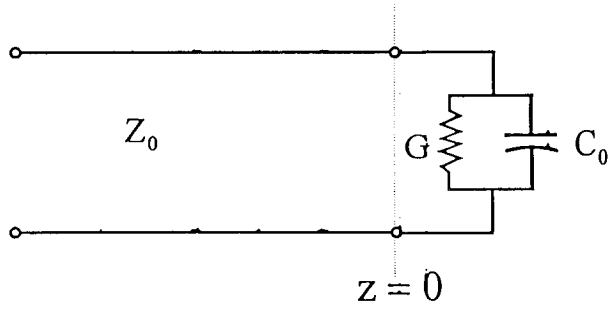

Fig. 2. The equivalent circuit of the cylindrical open-end microstrip line shown in Fig. 1.

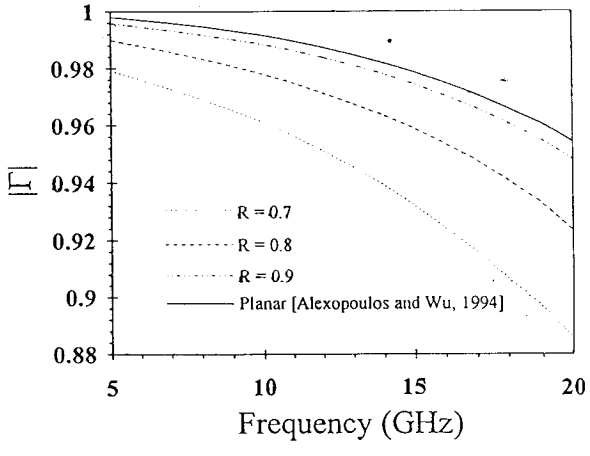

Fig. 3. The reflection coefficient magnitude at a cylindrical microstrip open-end discontinuity; ε_r=9.9, h=0.635 mm, W=0.635 mm.

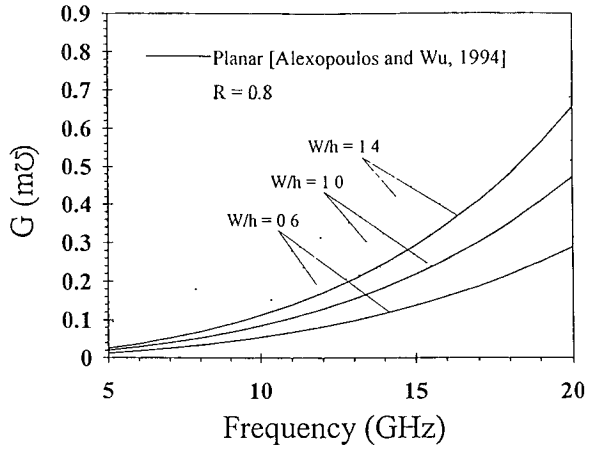

Fig. 4. The terminal conductance of an open-end cylindrical microstrip line; ε_r=9.9, h=0.635 mm

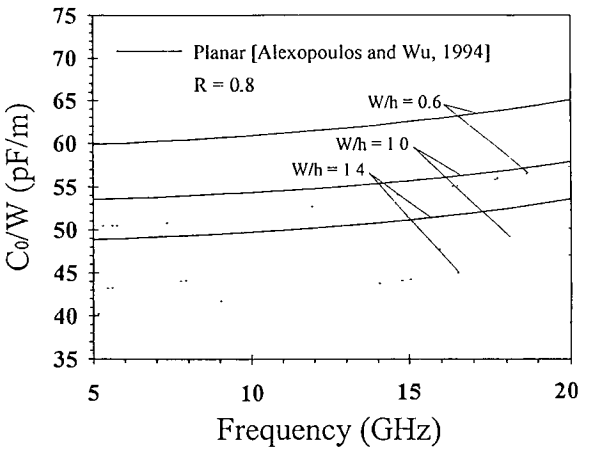

Fig. 5. The terminal capacitance of an open-end cylindrical microstrip line; ε_r=9.9, h=0.635 mm.

and Wu, 1994) are also shown for comparison. Different microstrip-line widths of W/h=0.6, 1.0, and 1.4 are presented. It is seen that the terminal conductance is larger for a cylindrical open-end microstrip line, as compared to the planar case, which suggests that the radiation and surface wave losses at a microstrip discontinuity increase when the curvature increases. The results for the terminal capacitance are presented in Fig. 5. It is found that the curvature decreases the terminal capacitance at a microstrip open-end discontinuity.

Finally, it should be noted that only the results for operating frequencies up to 20 GHz have been presented here. For higher frequencies, the wavelength of the wave propagating on the microstrip line becomes comparable or greater than the microstrip-line width and the substrate thickness. In this case, the $\hat{\phi}$ -directed current on the microstrip line should be considered, and the theoretical formulation and numerical computation will become much more complicated.

IV. Conclusions

The frequency-dependent characteristics of a cylindrical microstrip open-end discontinuity have been studied using full-wave analysis and moment-method calculation. The reflection coefficient, terminal conductance, and terminal capacitance for different stripline parameters have been calculated and discussed. Significant curvature effects on the characteristics of the cylindrical microstrip discontinuity have been observed. The accuracy of the theoretical results has also been checked, in a limiting case, with good agreement with the solutions of a planar open-end discontinuity case.

Acknowledgments

This work was supported by the National Science Council of the Republic of China under Grant NSC83-0404-E-110-017.

References

Alexopoulos, N. G. and A. Nakatani (1987) Cylindrical substrate microstrip line characterization. *IEEE Trans. Microwave Theory Tech.*, **35**, 843-849.

Alexopoulos, N. G. and S. C. Wu (1994) Frequency-independent equivalent circuit model for microstrip open-end and gap discontinuities. *IEEE Trans. Microwave Theory Tech.*, **42**, 1268-1272.

Harokopus, Jr., W. P., L. P. B. Katehi, W. Y. Ali-Ahmad and G. M. Rebeiz (1991) Surface wave excitation from open microstrip discontinuities. *IEEE Trans. Microwave Theory Tech.*, **39**, 1098-1107.

Jackson, R. W and D. M. Pozar (1985) Full-wave analysis of microstrip open-end and gap discontinuities. *IEEE Trans. Microwave Theory Tech.*, **33**, 1036-1042.

Ke, S. Y. and K. L. Wong (1994) Full-wave analysis of mutual coupling between cylindrical-rectangular microstrip antennas. *Microwave Opt. Technol. Lett.*, **7**, 419-421.

Kobayashi; M. and H. Sekine (1991) Closed-form expressions for the current distributions on open microstrip lines *IEEE Trans Microwave Theory Tech.*, **39**, 1115-1119.

Yang, H. Y., N. G. Alexopoulos and D. R. Jackson (1989) Microstrip open-end and gap discontinuities in a substrate-superstrate structure. *IEEE Trans. Microwave Theory Tech.*, **37**, 1542-1546.

Cylindrical Microstrip Discontinuities

柱面微帶線開路結構之全波理論分析

翁金輅　陳華明　蔡潤波

中山大學電機工程學系

摘　要

本文利用全波理論分析方法及動差法之數值運算，計算得到在柱面微帶線開路結構下之反射係數。並由計算得到之反射係數及該柱面微帶線之特性阻抗，我們可以得到一等效電路包含等效開路電導及等效開路電容，來模擬該開路結構。相關的數值結果在本文中有詳細討論。